Graefe's Arch Clin Exp Ophthalmol (2007) 245:855–862
DOI 10.1007/s00417-006-0475-3

LABORATORY INVESTIGATION

The efficacy of acrylic acid grafting and arginine–glycine–aspartic acid peptide immobilization on fibrovascular ingrowth into porous polyethylene implants in rabbits

Byung Woo Park · Hee Seok Yang · Se Hyun Baek · Kwideok Park · Dong Keun Han · Tae Soo Lee

Received: 1 June 2006 / Revised: 30 August 2006 / Accepted: 7 October 2006 / Published online: 22 November 2006

Abstract
Purpose To determine the effects of acrylic acid (AA) grafting by argon plasma treatment and of immobilization of arginine–glycine–aspartic acid (RGD) peptides on fibrovascular ingrowth rate into high-density porous polyethylene (HPPE) anophthalmic orbital implants.
Materials and methods Sixty rabbits were divided into three groups, with 20 rabbits in each group: (1) control group, rabbits implanted with unmodified HPPE; (2) PAA group, rabbits implanted with HPPE grafted with poly(AA) by argon plasma treatment; (3) RGD group, rabbits implanted with HPPE grafted with AA by argon plasma treatment and subsequently immobilized with RGD peptide. An HPPE spherical implant was put in the abdominal muscles of rabbit. After implantation for 4 weeks, the retrieved implants were sectioned and stained with hematoxylin and eosin (H&E). Blood vessels were counted using CD-31 immunostaining. Cross-sectional areas of fibrovascular ingrowth, blood vessel densities, and host inflammatory response scores were determined for all three groups.
Results The mean cross-sectional areas of fibrovascularization at 2 and 3 weeks after implantation were the greatest in the RGD group, followed by the PAA group. While minimal fibrovascular ingrowths were noted in all implants at 1 week, all the implants showed nearly complete ingrowth at 4 weeks. Blood vessel densities were the highest in the RGD group, followed by the PAA group at 2, 3, and 4 weeks. The mean inflammation scores of the PAA and RGD groups were less than that of the control group.
Conclusion Fibrovascularization into HPPE implants was enhanced by surface grafting of AA and further improved by immobilizing RGD peptides onto the grafted AA surfaces. The inflammatory reactions were mild by either technique of surface modification.

Keywords Anophthalmic implant · Medpor · Polyethylene · Surface modification · Acrylic acid · RGD · Fibrovascular ingrowth

B. W. Park
Yangpyeong First Eye Clinic,
Yangpyeong-gun, Gyeonggi-do, South Korea

H. S. Yang · K. Park · D. K. Han (✉)
Biomaterials Research Center,
Korea Institute of Science and Technology,
P.O. Box 131, Cheongryang,
Seoul 130-650, South Korea
e-mail: dkh@kist.re.kr

S. H. Baek
Department of Ophthalmology, Ansan Hospital, Korea University,
Ansan, Gyeonggi-do, South Korea

T. S. Lee (✉)
Department of Ophthalmology, Guro Hospital, Korea University,
Seoul 152-703, South Korea
e-mail: tsl98@unitel.co.kr

Introduction

High-density porous polyethylene (HPPE) has been successfully used in ophthalmology as an anophthalmic socket implant material [1–4], a lower eyelid spacer [5, 6], facial bone reconstruction [7], orbital fracture repair [8, 9], and volume augmentation [10]. It is believed that well-vascularized porous implants can reduce the incidence of implant migration and extrusion [11, 12]. However, implant exposure is the most common complications associated with porous anophthalmic implant surgery, though exposure rates vary [2, 13, 14].

Wound closure with tension, inadequate wound closure technique, infection, mechanical or inflammatory irritation, and delayed ingrowth of fibrovascular tissue with subsequent tissue breakdown have been pointed out to predis-

pose anophthalmic implants to exposure [15, 16]. Fibrovascular ingrowth into porous implants provides anchorage, which limits migration and extrusion, and is perceived to lower the incidence of infection [10, 12, 17]. Moreover, it is well known that enhanced fibrovascular ingrowth reduces the incidence of porous orbital implant exposure. In this study, we aimed to determine the efficacy of two techniques of surface modification on enhancing fibrovascular ingrowth into HPPE anophthalmic orbital implants, by (1) surface grafting HPPE implants with acrylic acid (AA) by argon plasma treatment and (2) immobilizing arginine–glycine–aspartic acid (RGD) peptides on the surfaces of AA grafted HPPE implants. The grafting of AA onto HPPE by cold plasma treatment using argon gas increases surface hydrophilicity, due to the introduction of the AA carboxyl group [18, 19]. Increasing surface hydrophilicity of biomaterials can enhance cell attachment and proliferation [19, 20]. RGD peptide is an essential cell adhesion peptide sequence that is found in many extracellular matrix proteins [21], and, thus, immobilization of RGD peptides on biomaterial surface has been shown to promote cellular adhesion and growth [22, 23].

In our previous work, the hydrophilicity of surface-modified polyethylene (PE) samples was increased through plasma treatment and AA grafting, as confirmed by our measuring water contact angles. Fibroblast adhesion and proliferation on the surface-modified PEs were significantly improved during in vitro culture. In this study, to evaluate the efficacy of two techniques of surface modification on fibrovascular ingrowth rate into HPPE anophthalmic orbital implants, we performed an animal study with a rabbit model. Cross-sectional areas of fibrovascular ingrowth, host inflammatory response scores, and blood vessel densities were determined and compared in three test groups: unmodified HPPE (control group), AA-grafted HPPE (PAA group), and RGD-immobilized HPPE (RGD group).

Materials and methods

Sixty female albino New Zealand rabbits, weighing approximately 3 kg, were implanted with HPPE (Medpor, Porex Surgical, GA, USA) spherical implants (12 mm in diameter) between abdominal muscle layers, as described in the study by Rubin et al. [24]. Rabbits were divided into three groups of 20: (1) control group, rabbits implanted with unmodified HPPE; (2) PAA group, rabbits implanted with HPPE grafted with poly(AA) by argon plasma treatment; (3) RGD group, rabbits implanted with HPPE grafted with AAs by argon plasma treatment and subsequently immobilized with RGD peptide.

The hydrophilization of HPPE by AA grafting and the subsequent immobilization of RGD peptides were undertaken with plasma treatment. HPPE spheres were placed in the chamber of the plasma treatment system (IDT Engineering, Bucheon, Korea). The chamber was pumped down to 10 mTorr to remove air, moisture, and methyl alcohol. Argon was fed into the chamber when the pressure became 200 mTorr. Argon gas plasma was given at 50 W for 4 min, and the chamber was pumped down again to 20 mTorr. AA was fed into the chamber when the pressure became 200 mTorr, and then plasma was given at 50 W for 4 min. The fabricated AA-grafted PE (PE-g-PAA; PAA group) was washed with methyl alcohol to remove the unreacted AA.

After plasma treatment with grafting of AA, the HPPE sphere was immersed in 10 ml of 1-ethyl-3-(dimethylaminopropyl)-carbodiimide (EDC) in MES buffer (50 mg EDC, pH 4.6) in room temperature for 4 h with mild stirring to activate carboxyl groups. The activated HPPE was immersed in 10 ml of glycine–arginine–glycine–aspartic acid (GRGD; Anygen Co., Gwangju, Korea) in phosphate-buffered saline (PBS; 4.04 mg, pH 7.4) solution at room temperature for 2 h with mild stirring. The RGD-immobilized HPPE sphere (PE-g-PAA-RGD; RGD group) was rinsed with PBS solution for 15 min, distilled water for 5 min, MES buffer solution for 10 min, and distilled water for 10 min again.

For the animal study, the rabbits were anesthetized with an intramuscular injection of ketamine (25 mg/kg body weight) into the thigh. A mixture of 1% lidocaine and 1:100,000 epinephrine was then injected locally, as a supplementary measure and to aid hemostasis. A vertical incision of 2 cm in length was made in the right abdominal wall. Once the abdominal muscles were exposed, the HPPE sphere was implanted between the layers of abdominal muscles, approximately 3 cm lateral from the incision site. After securing the implant in position, we closed the overlying muscle layer and skin with 4-0 Vicryl sutures in separate layers. Gentamicin sulfate (5 mg/kg per day) was injected intramuscularly into the thigh after the surgery, and this was repeated daily up to 5 days postoperatively.

Implants were harvested from five rabbits in each group at 1, 2, 3, and 4 weeks, postoperatively. Implants were immediately fixed in 10% formalin solution, embedded in a paraffin block and sectioned at the equator (12 mm in diameter). Sections were, stained with hematoxylin and eosin (H&E) and immunostained for CD-31 (an endothelial cell marker). Immunostaining was performed with a labeled streptavidin biotin kit (DAKO, Glostrup, Denmark). Anti CD-31 antibody (DAKO) was used in a dilution of 1:20, and Mayer's hematoxylin was used as a counterstain. Two pathologists at Guro Hospital who were unaware of the purpose of this study examined the histopathologic sections.

H&E-stained sections were scanned (Scanjet 4070c, Hewlett-Packard, CA, USA) to produce digital photographs

(×1 magnification), and Adobe Photoshop CS (Adobe systems, CA, USA), was used to overlay 64 radial lines from the centers of the sectioned spherical implants on the photographs. For each radial line, the innermost point reached by fibrovascular tissue was marked, and lines were then drawn to connect the points on adjacent radial lines (Fig. 1). When the boundaries of the spherical implant were then drawn, ImageJ 1.32j (NIH, MD, USA) software was used to calculate the percentage of the cross-sectional area of fibrovascular ingrowth compared with the entire cross-sectional area of implants.

CD-31 expression was evaluated at 1 mm from the surface of the HPPE spheres at the 3, 6, 9, and 12 o'clock positions. The numbers of capillaries expressing CD-31 were counted, and the results from the four separate fields were averaged. Host inflammatory response was scored using a modification of the system described by Kossovsky et al. [25]. Implants were divided into outer zone (<3 mm from the implant surface) and inner zone (>3 mm). The highest score from each kind of cell was assigned for each zone (Table 1). The average cross-sectional area of ingrowth, number of CD-31 expressing capillaries, and host inflammatory response score were calculated for each group. The SPSS 12.0 for Windows was used for the statistical analysis. A p value less than 0.05 was considered statistically significant.

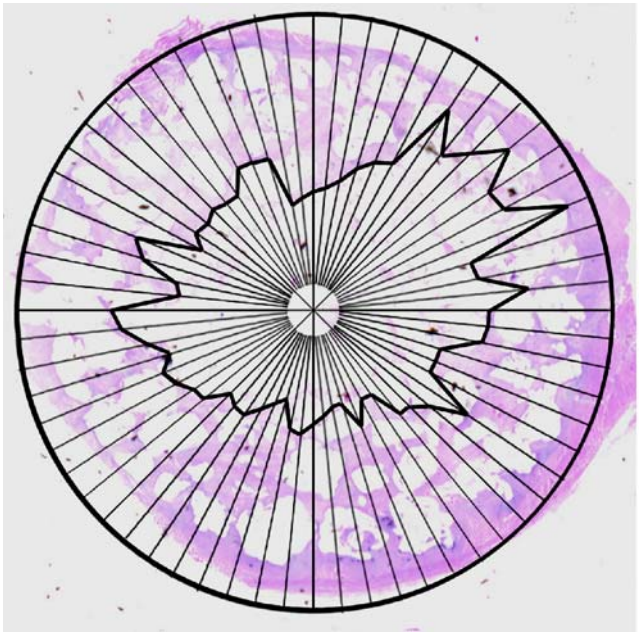

Fig. 1 Measurement of the cross-sectional area of fibrovascular ingrowth into the spherical PE implants. Sixty four radial lines from the centers of sectioned spherical implants were overlaid on the photographs of implants stained with H&E. For each radial line, the innermost point reached by fibrovascular tissue was marked and the lines were then drawn to connect the points on the adjacent radial lines

Table 1 Scoring system for host inflammatory response to implant. The cell count indicates the number of cells in the x200 magnification field under light microscopy

Scale	
0	No cells
1	1–20 cells
2	21–50 cells
3	More than 50 cells
Score	
Acute inflammation	
Polymorphonuclear cells (0–3)	
Chronic inflammation	
Eosinophils (0–3)	
Lymphocytes (0–3)	
Plasma cells (0–3)	
Macrophages (0–3)	
Giant cells (0–3)	

Results

All rabbits were raised under the same conditions and endured the implants well. Complications such as migration, exposure, or abscess formation were not noted at the times of retrieval. No fibrous capsule formation around implants was found grossly in any PE sphere explanted at 1 week after implantation. However, scant fibrovascular ingrowth was observed microscopically. Thin fibrous capsules surrounded implants explanted at 2, 3, and 4 weeks, especially in those at 4 weeks. Implants at 4 weeks showed nearly complete fibrovascular ingrowth. Typical examples of histological features are demonstrated in Fig. 2. Mean percentage areas of fibrovascular ingrowth in each group are shown in Table 2. At 2 and 3 weeks after implantation, the mean areas of fibrovascular ingrowth were the greatest in the RGD group (22.3±4.0% at 2 weeks; 66.1±11.5% at 3 weeks), followed by the PAA group (22.2 ±3.3% at 2 weeks; 59.4±9.6% at 3 weeks) and the control group (14.2±2.7% at 2 weeks; 47.6±8.8% at 3 weeks). Significant differences were observed among the three groups in terms of the areas of fibrovascular ingrowth at 2 and 3 weeks (Kruskal–Wallis test, p=0.009 at 2 weeks; p=0.034 at 3 weeks; p=0.580 at 4 weeks). Significant differences were observed between the PAA and control groups at 2 and 3 weeks (Mann–Whitney U test, p=0.009 at 2 weeks; p=0.028 at 3 weeks; p=0.914 at 4 weeks, multiple comparison). Significant differences were also found between the RGD and control groups at 2 and 3 weeks (Mann–Whitney U test, p=0.009 at 2 weeks; p=0.028 at 3 weeks; p=0.316 at 4 weeks), but no significant difference in ingrowth area was observed between the RGD and PAA groups throughout the study (Mann–Whitney U test, p=0.834 at 2 weeks; p=0.602 at 3 weeks; p=0.435 at 4 weeks).

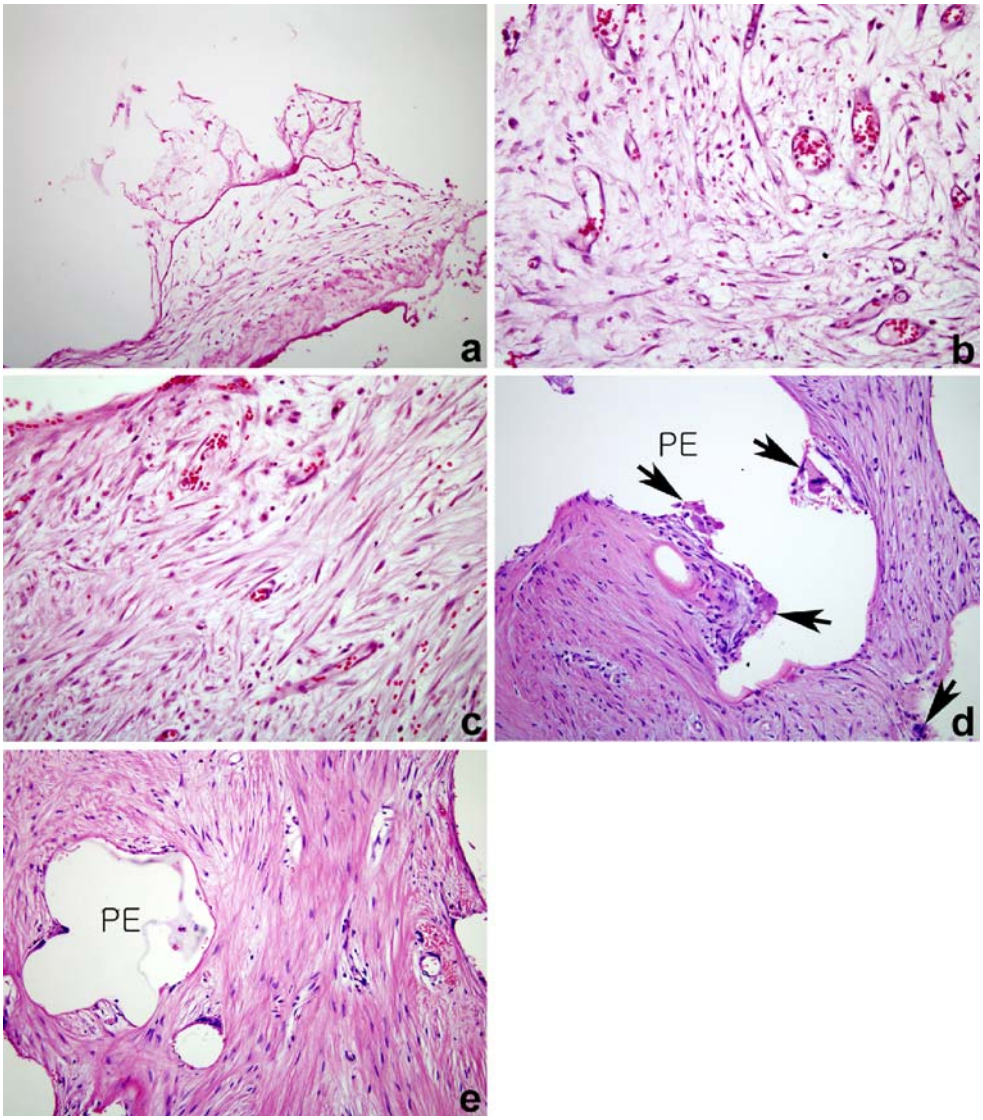

Fig. 2 Histology of H&E staining. **a** Microscopic observation of new tissue at the periphery of porous PE implant in the control group explanted at 1 week (×200). **b** Control group at 2 weeks. Randomly aligned spindle-shaped fibroblasts and scattered capillaries were found in loose connective tissue (×400). **c** PAA group at 2 weeks. Some fibroblasts begun to align, but connective tissue was not dense (×400). **d** Control group at 3 weeks. Fibroblasts were dense, and aligned and scattered giant cells were lined at the tissue–PE interface (*arrows*) (×200). **e** RGD group at 4 weeks. Dense collagen bands are shown (×200)

The mean numbers of CD-31 positive blood vessels and an example of CD-31 immunostaining are shown in Table 3 and Fig. 3, respectively. At 2, 3, and 4 weeks after implantation, the numbers of CD-31 positive blood vessels were the largest in the RGD group (23.1±1.87 at 2 weeks; 33.7±4.5 at 3 weeks; 40.6±2.7 at 4 weeks), followed by the PAA group (15.4±6.3 at 2 weeks; 28.4±6.5 at 3 weeks; 35.0±3.8 at 4 weeks) and the control group (9.9±2.1 at 2 weeks; 13.5±1.4 at 3 weeks; 23.3±1.5 at 4 weeks). Differences were significant in the numbers of CD-31 positive blood vessels among the three groups (Kruskal–Wallis test, p=0.012 at 2 weeks; p=0.007 at 3 weeks; p=0.003 at 4 weeks). Between the PAA and control groups, the differences were significant at 3 and 4 weeks (Mann–Whitney U test, p=0.117 at 2 weeks; p=0.009 at 3 weeks; p=0.009 at 4 weeks). Between the RGD and control groups, the differences were also significant at 2, 3, and 4 weeks (Mann–Whitney U test, p=0.009 at 2 weeks; p=0.009 at 3 weeks; p=0.009 at 4 weeks). The differences between the RGD and PAA groups were significant at 2 and 4 weeks (Mann–Whitney U test, p=0.047 at 2 weeks; p=0.251 at 3 weeks; p=0.028 at 4 weeks).

Mean host inflammatory response scores are shown in Table 4. Inflammation was mild in all groups. Of the inflammatory cells, polymorphonuclear cells were predominant at 1 week, but giant cells and eosinophils became predominant from 2 weeks. The PAA and RGD groups had lower inflammation scores than the control group on average, and the PAA group had the lowest inflammation scores at 3 and 4 weeks.

Discussion

Many studies have shown that porous anophthalmic orbital implants permit fibrovascular ingrowth from the surrounding tissues [3, 24, 26]. This integration between implant and host tissue reduces postoperative complications such as

Table 2 Cross-sectional area of fibrovascular ingrowth into 12 mm porous polyethylene implants over time. The percentage of fibrovascular ingrowth was based on the ratio of the cross-sectional area of fibrovascular ingrowth compared with the entire cross-sectional area of implants

Implantation time (weeks)	Fibrovascular ingrowth (%)		
	Control[a]	PAA[b]	RGD[c]
1	0	0	0
2	14.2±2.7	22.2±3.3	22.3±4.0
3	47.6±8.8	59.4±9.6	66.1±11.5
4	93.5±7.4	95.0±5.0	98.5±3.4

[a] Control. Rabbits implanted with unmodified HPPE
[b] PAA. Rabbits implanted with HPPE that was grafted with AA by argon plasma treatment
[c] RGD. Rabbits implanted with HPPE grafted with AA by argon plasma treatment and subsequently immobilized with RGD peptide

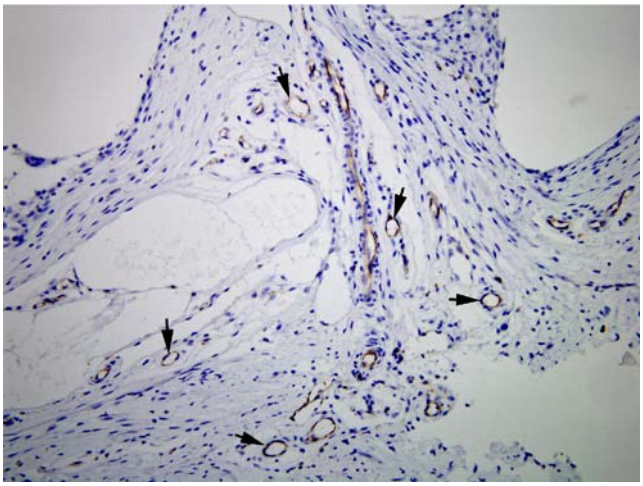

Fig. 3 Immunostaining of CD-31 for RGD group at 4 weeks (×200). Staining of endothelial cells, shows representative capillary vessels (*arrows*)

migration, infection, or extrusion [10, 12, 17]. In addition, the direct coupling of an ocular prosthesis to a porous, vascularized implant can provide greater prosthesis motility [11, 27]. Materials currently available for porous implants are HPPE (Medpor, USA), coralline HA (Bio-Eye, Integrated Orbital Implants, SD, USA), synthetic HA (FCI Ophthalmics, Issy-Les-Moulineaux, France), and aluminum oxide (Bioceramic implant, FCI Ophthalmics, Issy-Les-Moulineaux, France). HPPE is an inert, white, ultra-high-density material that has been used as an alloplastic implant in humans since the 1940s [28]. It has an extensive system of interconnected channels through the implant, ranging in size from 125 μm to 1,000 μm [26, 29]. It is relatively inexpensive and has high tensile strength, malleability, and biocompatibility [26, 30]. Its surface is smoother than that of HA or aluminum oxide, which results in less tissue breakdown by friction. It is not brittle and is easily processable. Moreover, sutures can be used through these implants [2, 4].

Table 3 Mean number of CD-31 positive blood vessels. The expression of CD-31 was evaluated at 1mm into the PE spheres at the 3, 6, 9, and 12 o'clock positions under ×200 magnification. The numbers of CD-31 expressed capillaries were counted and averaged

Implantation time (weeks)	Control[a]	PAA[b]	RGD[c]
2	9.9±2.1	15.4±6.3	23.1±1.9
3	13.5±1.4	28.4±6.5	33.7±4.5
4	23.3±1.5	35.0±3.8	40.6±2.7

[a] Control. Rabbits implanted with unmodified HPPE
[b] PAA. Rabbits implanted with HPPE that was grafted with AA by argon plasma treatment
[c] RGD. Rabbits implanted with HPPE grafted with AA by argon plasma treatment and subsequently immobilized with RGD peptide

Studies on fibrovascular ingrowth into porous orbital implants have been performed by many authors [2, 26, 31–34], who have primarily addressed chemical compositions [26, 33], pore sizes [3, 33], wrapping [35], vascularity of recipient tissue [35], fenestration [3], and the use of growth factors [26, 31, 35]. Our study presents the results of the application of new surface hydrophilization techniques:

Table 4 Host inflammatory response scores for porous polyethylene implants. Scores are the averages for each group. *N/A* not assessed because of poor fibrovascular ingrowth into the inner halves at 1 and 2 weeks

Implantation time (weeks)	Implant	Chronic inflammation score		Acute inflammation score	
		Outer half	Inner half	Outer half	Inner half
1	Control[a]	0	N/A	1.4	N/A
	PAA[b]	0	N/A	1.2	N/A
	RGD[c]	0	N/A	1.2	N/A
2	Control	1.4	N/A	0.6	N/A
	PAA	1.4	N/A	0.2	N/A
	RGD	1.4	N/A	0.2	N/A
3	Control	3.6	1.2	0.2	0
	PAA	2.8	1.25	0.4	0.25
	RGD	3.2	1.4	0.2	0
4	Control	3.6	3.4	0	0
	PAA	2.2	2.2	0	0
	RGD	3.0	2.8	0	0

[a] Control. Rabbits implanted with unmodified HPPE
[b] PAA. Rabbits implanted with HPPE that was grafted with AA by argon plasma treatment
[c] RGD. Rabbits implanted with HPPE grafted with AA by argon plasma treatment and subsequently immobilized with RGD peptide

surface grafting of acrylic acid and the subsequent immobilization of RGD peptide on the modified surface.

Plasma treatment is recognized as an effective way of modifying surfaces and is attracting more interest in biomedical research. Plasma treatment with appropriate monomers can change surface characteristics, such as wettability (hydrophilicity or hydrophobicity), metal adhesion, dyeability, refractive index, hardness, chemical inertness, lubricity, and biocompatibility [36]. Plasmas are typically obtained when gases are excited into high-energy states by radiofrequency or microwave radiation, or by electrons from a hot filament discharge. High densities of ionized and excited species change the surface properties of inert materials [36]. Plasma-based techniques that combine the advantages of conventional plasma and ion beam technologies are effective for modifying the surfaces of medical implants with complex shapes [37], without altering their bulk properties. Khang et al. [38] observed that fibroblasts adhered, spread, and grew more on moderately hydrophilic poly(L-lactide-co-glycolide) (PLGA) surfaces than on more hydrophobic or hydrophilic positions, at a water contact angle of 55°. Lee et al. [39] concurred that more endothelial cells adhered to the regions of moderate hydrophilicity on the corona discharge-treated PE than to more hydrophobic or hydrophilic positions, and maximum adhesion was observed at the contact angles of 55°.

In the previous study, the water contact angles of control PE, AA-grafted PE and RGD-immobilized PE films were 105°, 50°, and 60°, respectively, which demonstrated the hydrophilized surface via two surface modification methods (unpublished data). The decreased contact angles are close to those of the previous reports that showed maximum cell adhesion at 55° [38, 39]. The measurement of cell density was carried out with a cell proliferation reagent, WST-1 (Roche Diagnostic, Penzberg, Germany) at 12 h, 24 h, and 72 h after inoculation. When the absorbance at 450 nm was measured with an enzyme-linked immunosorbent assay (ELISA) reader, the cell density was highest with the RGD-immobilized PE, followed by AA-grafted PE and control PE. On the basis of these results, the authors could expect that these surface modifications could promote fibrovascular ingrowth into HPPE implants in vivo as well. Some studies have reported that biomaterials grafted with AA by plasma treatment, which involves the attachment of surface carboxylic acid groups, improve cell adhesion and proliferation. Kim and Seo [18] hydrophilized the PE surface by grafting AA using cold argon plasma treatment, whereas Yang et al. [19] hydrophilized poly(L-lactic acid) (PLLA) using plasma glow discharge treatment to graft carboxylic acid containing monomers, such as AA, maleic acid, itaconic acid, and trans-acotinic acid. These hydrophilized PLLA films and three-dimensional scaffolds containing surface carboxylic acids improved fibroblast adhesion and proliferation.

RGD sequence is often used as a peptide sequence for stimulating cell adhesion to synthetic surfaces [40]. RGD peptides were first identified by Pierschbacher and Ruoslahti as the minimal cell adhesion peptide sequence in fibronectin [41]. Many other cell adhesive RGD sequences have since been identified in other extracellular matrix proteins, including vitronectin, fibronectin, von Willebrand factor, collagen, laminin, osteopontin, tenascin and bone sialoprotein, and in membrane proteins, viral and bacterial proteins, and snake venoms (neurotoxins and disintegrins) [21]. The RGD sequences of each adhesive protein are recognized by at least one member of a family of structurally related cell membrane receptors, the integrins, which are heterodimeric proteins possessing two membrane-spanning subunits. As cell adhesion receptors, integrins play an important role in controlling various steps in the signaling pathways that regulate processes as diverse as proliferation, differentiation, and apoptosis. During migration, cells move on the extracellular matrix using integrins, and immobilization of RGD peptides on the surfaces of biomaterials contributes to increasing cellular adhesion and growth [22, 23]. In this sense, AA and RGD peptide surface treatment could help early fibrovascular ingrowth into porous PE implants both in vitro and in vivo.

Hersel et al. [40] pointed out that biomaterial coatings containing cell adhesive proteins such as EGF and bFGF have disadvantages in terms of medical application. Proteins have to be isolated from organisms and purified, and, thus, there are risks of undesirable immune responses or infection. Proteins are also subject to proteolytic degradation and, thus, cannot be used in long-term. However, cell recognition motifs as small immobilized peptides may be stable under sterilization conditions, heat treatment, pH variation, and storage. On the fibroblast cultures in the previous work, both techniques of surface modification provided better fibroblast adhesion and proliferation than did the unmodified control. The RGD-immobilized surface was more effective than AA grafting was. Thus, it was postulated that early fibrovascularization could be induced by the modified surfaces.

In the present study, an in vivo rabbit abdominal muscle model was used, as described by Rubin et al. [24]. Intraoperative and postoperative complications can be lessened, owing to the simplicity of its surgical procedure. It is recognized that the abdominal muscle may not provide the same environment as the ocular tissue does. However, it is possible that the present in vivo data from the implants in the abdominal muscle could be extrapolated for the results in the ocular tissue. All rabbits tolerated the implants well, with no complications. Only scant microscopic ingrowths were noted in all groups at 1 week after implantation. At

4 weeks, all implants showed nearly complete fibrovascular ingrowth, and no statistical differences were observed in terms of fibrovascular ingrowth areas. However, we found more active vascular ingrowths in the PAA and RGD groups than in the control group at 4 weeks, as identified by the results of CD-31 immunostaining. In the report of the use of a rabbit model, Rubin et al. described that cross-sectional ingrowth at 6 weeks was 74% with 16 mm spherical HPPE implants [24]. Although direct comparison was difficult, because of the size difference, all the 12 mm implants showed nearly complete fibrovascular ingrowth at 4 weeks in this study. Long-term efficacy of current surface modifications may be clearly evaluated with larger implants used in the future studies.

The grafting of AA and the surface immobilization of RGD facilitated fibrovascular ingrowth into the spherical HPPE implants at 2 and 3 weeks. Moreover, regions of fibrovascular ingrowth were broader with the RGD immobilization than with the AA grafting. CD-31 is a platelet endothelial cell adhesion molecule of the IgG family and has been a sensitive marker for vascular endothelial cells specifically, but not for lymphatic endothelium [42]. The numbers of CD-31 positive vessels were found to be significantly greater in the PAA and RGD groups, especially more in the RGD group. Because CD-31 is a sensitive marker of vascular endothelial cell, it is supposed to reveal the cellularity as well as the distribution of endothelial cells in the fibrovascularized tissue grown on the implant. Vascularization into the porous implant began at the periphery and proceeded into the center. Increased numbers of vessels are critical to fibrovascularization on the implants, which is believed to reduce infection, extrusion, and exposure of the implant. The presence of vascularized host tissue in and around the implant gave physical stability as well as resistance to infection of either expanded polytetrafluoroethylene (e-PTFE, Gore-Tex) or HPPE implants in rats [43].

Only mild degrees of inflammation were observed in all of the groups. The PAA and RGD groups showed less inflammation than did the control group. It is not clear at this time why the RGD group showed a higher inflammatory response score than the PAA group did. Kao et al. [44] observed that PEG-based networks grafted with RGD-containing peptide retained higher levels of adherent macrophages than the surfaces grafted with other peptides. It might be due to the difference in affinity of RGD motifs to inflammatory cells.

Conclusion

Fibrovascular ingrowth into HPPE implants could be improved by the use of (1) hydrophilization of HPPE surfaces with AA by argon plasma treatment, and (2) AA grafting and subsequent RGD peptide immobilization on the AA grafted surface. Blood vessel density was higher in the RGD-immobilized HPPE than in the AA-grafted HPPE at 2 and 4 weeks after implantation. Inflammatory responses to the surface-modified HPPE implants were milder than those of unmodified HPPE. The present surface modification can promote fibrovascular ingrowth into HPPE implants and may contribute to reducing the rate of exposure after anophthalmic socket implant surgery.

Acknowledgement This work was supported by KIST grant 2E19220 from Ministry of Science and Technology, Korea. The authors are grateful to two pathologists, Ju-Han Lee and Ji-Hye Lee at Department of Pathology, School of Medicine, Korea University, who examined the histopathological sections.

References

1. De Potter P, Duprez T, Cosnard G (2000) Postcontrast magnetic resonance imaging assessment of porous polyethylene orbital implant (Medpor). Ophthalmology 107:1656–1660
2. Blaydon SM, Shepler TR, Neuhaus RW, White WL, Shore JW (2003) The porous polyethylene (Medpor) spherical orbital implant: a retrospective study of 136 cases. Ophthal Plast Reconstr Surg 19:364–371
3. Rubin PA, Popham JK, Bilyk JR, Shore JW (1994) Comparison of fibrovascular ingrowth into hydroxyapatite and porous polyethylene orbital implants. Ophthal Plast Reconstr Surg 10:96–103
4. Karesh JW, Dresner SC (1994) High-density porous polyethylene (Medpor) as a successful anophthalmic socket implant. Ophthalmology 101:1688–1695
5. Morton AD, Nelson C, Ikada Y, Elner VM (2000) Porous polyethylene as a spacer graft in the treatment of lower eyelid retraction. Ophthal Plast Reconstr Surg 16:146–155
6. Wong JF, Soparkar CN, Patrinely JR (2001) Correction of lower eyelid retraction with high density porous polyethylene: the Medpor lower eyelid spacer. Orbit 20:217–225
7. Romano JJ, Iliff NT, Manson PN (1993) Use of Medpor porous polyethylene implants in 140 patients with facial fractures. J Craniofac Surg 4:142–147
8. Ng SG, Madill SA, Inkster CF, Maloof AJ, Leatherbarrow B (2001) Medpor porous polyethylene implants in orbital blowout fracture repair. Eye 15:578–582
9. Choi JC, Fleming JC, Aitken PA, Shore JW (1999) Porous polyethylene channel implants: a modified porous polyethylene sheet implant designed for repairs of large and complex orbital wall fractures. Ophthal Plast Reconstr Surg 15:56–66
10. Rubin PA, Bilyk JR, Shore JW (1994) Orbital reconstruction using porous polyethylene sheets. Ophthalmology 101:1697–1708
11. Perry AC (1990) Integrated orbital implants. Adv Ophthalmic Plast Reconstr Surg 8:75–81
12. Rosen HM (1991) The response of porous hydroxyapatite to contiguous tissue infection. Plast Reconstr Surg 88:1076–1080
13. Remulla HD, Rubin PA, Shore JW, Sutula FC, Townsend DJ, Woog JJ, Jahrling KV (1995) Complications of porous spherical orbital implants. Ophthalmology 102:586–593
14. Sagoo MS, Olver JM (2004) Autogenous temporalis fascia patch graft for porous polyethylene (Medpor) sphere orbital implant exposure. Br J Ophthalmol 88:942–946

15. Jordan DR, Bawazeer A (2001) Experience with 120 synthetic hydroxyapatite implants (FCI3). Ophthal Plast Reconstr Surg 17:184–190
16. Rosen HM, McFarland MM (1990) The biologic behavior of hydroxyapatite implanted into the maxillofacial skeleton. Plast Reconstr Surg 85:718–723
17. Merritt K, Shafer JW, Brown SA (1979) Implant site infection rates with porous and dense materials. J Biomed Mater Res 13:101–108
18. Kim MJ, Seo ED (2002) Immobilization and grafting of acrylic acid on polyethylene surface by Ar-plasma treatment. Polymer (Korea) 26:279–286
19. Yang HS, Ahn KD, Han DK (2004) Surface properties and cell adhesion behaviors of PLLA films and dual pore scaffolds grafted with carboxyl acid. Biomater Res 8:135–142
20. Khang G, Lee SJ, Jeon JH, Lee JH, Lee HB (2000) Interaction of fibroblast cell onto physicochemically treated PLGA surfaces. Polymer (Korea) 24:869–876
21. Ruoslahti E, Pierschbacher MD (1987) New perspectives in cell adhesion: RGD and integrins. Science 238:491–497
22. Burdick JA, Anseth KS (2002) Photoencapsulation of osteoblasts in injectable RGD-modified PEG hydrogels for bone tissue engineering. Biomaterials 23:4315–4323
23. Massia SP, Hubbell JA (1991) Human endothelial cell interactions with surface-coupled adhesion peptides on a nonadhesive glass substrate and two polymeric biomaterials. J Biomed Mater Res 25:223–242
24. Rubin PA, Nicaeus TE, Warner MA, Remulla HD (1997) Effect of sucralfate and basic fibroblast growth factor on fibrovascular ingrowth into hydroxyapatite and porous polyethylene alloplastic implants using a novel rabbit model. Ophthal Plast Reconstr Surg 13:8–17
25. Kossovsky N, Millett D, Juma S, Little N, Briggs PC, Raz S, Berg E (1991) In vivo characterization of the inflammatory properties of poly(tetrafluoroethylene) particulates. J Biomed Mater Res 25:1287–1301
26. Jordan DR, Brownstein S, Dorey M, Yuen VH, Gilberg S (2004) Fibrovascularization of porous polyethylene (Medpor) orbital implant in a rabbit model. Ophthal Plast Reconstr Surg 20:136–143
27. Guillinta P, Vasani SN, Granet DB, Kikkawa DO (2003) Prosthetic motility in pegged versus unpegged integrated porous orbital implants. Ophthal Plast Reconstr Surg 19:119–122
28. Anderson RL, Thiese SM, Nerad JA, Jordan DR, Tse D, Allen L (1990) The universal orbital implant: indications and methods. Adv Ophthalmic Plast Reconstr Surg 8:88–99
29. Mawn LA, Jordan DR, Gilberg S (1998) Scanning electron microscopic examination of porous orbital implants. Can J Ophthalmol 33:203–209
30. Sarvananthan N, Liddicoat AJ, Fahy GT (1999) Synthetic hydroxyapatite orbital implants: a clinical and MRI evaluation. Eye 13:205–208
31. Nicaeus TE, Tolentino MJ, Adamis AP, Rubin PA (1996) Sucralfate and basic fibroblast growth factor promote endothelial cell proliferation around porous alloplastic implants in vitro. Ophthal Plast Reconstr Surg 12:235–239
32. Wang JS, Aspenberg P (1996) Basic fibroblast growth factor promotes bone ingrowth in porous hydroxyapatite. Clin Orthop Relat Res 333:252–260
33. Bigham WJ, Stanley P, Cahill JM Jr, Curran RW, Perry AC (1999) Fibrovascular ingrowth in porous ocular implants: the effect of material composition, porosity, growth factors, and coatings. Ophthal Plast Reconstr Surg 15:317–325
34. Sabini P, Sclafani AP, Romo T 3rd, McCormick SA, Cocker R (2000) Modulation of tissue ingrowth into porous high-density polyethylene implants with basic fibroblast growth factor and autologous blood clot. Arch Facial Plast Surg 2:27–33
35. Soparkar CN, Wong JF, Patrinely JR, Davidson JK, Appling D (2000) Porous polyethylene implant fibrovascularization rate is affected by tissue wrapping, agarose coating, and insertion site. Ophthal Plast Reconstr Surg 16:330–336
36. Chu PK, Chen JY, Wang LP, Huang N (2002) Plasma-surface modification of biomaterials. Mater Sci Eng R 36:143–206
37. Chim H, Ong JL, Schantz JT, Hutmacher DW, Agrawal CM (2003) Efficacy of glow discharge gas plasma treatment as a surface modification process for three-dimensional poly (D,L-lactide) scaffolds. J Biomed Mater Res 65A:327–335
38. Khang G, Lee SJ, Lee JH, Kim YS, Lee HB (1999) Interaction of fibroblast cells on poly(lactide-co-glycolide) surface with wettability chemogradient. Biomed Mater Eng 9:179–187
39. Lee JH, Lee SJ, Khang G, Lee HB (2000) The effect of fluid shear stress on endothelial cell adhesiveness to polymer surfaces with wettability gradient. J Colloid Interface Sci 230:84–90
40. Hersel U, Dahmen C, Kessler H (2003) RGD modified polymers: biomaterials for stimulated cell adhesion and beyond. Biomaterials 24:4385–4415
41. Pierschbacher MD, Ruoslahti E (1984) Cell attachment activity of fibronectin can be duplicated by small synthetic fragments of the molecule. Nature 309:30–33
42. Sclafani AP, Thomas JR, Cox AJ, Cooper MH (1997) Clinical and histologic response of subcutaneous expanded polytetrafluoroethylene (Gore-Tex) and porous high-density polyethylene (Medpor) implants to acute and early infection. Arch Otolaryngol Head Neck Surg 123:328–336
43. Horak ER, Leek R, Kl\enk N, LeJeune S, Smith K, Stuart N, Greenall M, Stepniewska K, Harris AL (1992) Angiogenesis, assessed by platelet/endothelial cell adhesion molecule antibodies, as indicator of node metastases and survival in breast cancer. Lancet 340:1120–1124
44. Kao WJ, Hubbell JA, Anderson JM (1999) Protein-mediated macrophage adhesion and activation on biomaterials: a model for modulating cell behavior. J Mater Sci Mater Med 10:601–605